Thermodynamic properties of the attractive Hubbard model

Alain Sewer[1,2] and Hans Beck[2]

[1]*Institut Romand de Recherche Numérique en Physique des Matériaux (IRRMA), EPFL, 1015 Lausanne, Switzerland*
[2]*Institut de Physique, Université de Neuchâtel, 2000 Neuchâtel, Switzerland*

We study the thermodynamic properties of short coherence length superconductors in the pseudogap phase. Our description is based on the attractive Hubbard model that reproduces well these features in the intermediate coupling regime ($U = 4t$). Basing ourselves on the self-consistent T-matrix approximation, we perform an analytical calculation that yields an expression for the thermodynamic grand potential of the electronic system. It shows that the relevant degrees of freedom above the critical temperature are well-defined bosonic fluctuations describing virtual Cooper pairing. The latter are described by the low-energy expansion of the T matrix whose evaluation reveals that these pairing fluctuations behave quite similarly to free bosons undergoing a Bose-Einstein condensation (BEC). We then carefully analyze the conditions allowing for this interpretation and finally consider the case of underdoped high-temperature superconductors where typical BEC features have been observed experimentally.

I. INTRODUCTION

High-temperature cuprate superconductors are known to have various remarkable and intriguing properties even in their normal state. Thermodynamic quantities as well as transport coefficients deviate from Fermi-liquid behavior, and electronic spectral functions show strong precursor behavior when the critical temperature T_c is approached. The transition to the superconducting state itself is characterized by strong fluctuations—unobservable in traditional superconductors, which are well described by BCS theory.

In this context we are particularly interested in the following features:

(1) The specific heat c_V is an interesting indicator for the nature of the superconducting transition and for the type of fluctuations that accompany the latter. The experimental data[1] show rather different features for different materials. For traditional low-temperature superconductors c_V has a jump at T_c as predicted by the BCS theory. In an applied magnetic field, the jump follows the field-dependent critical temperature and gradually loses its sharpness. For $YBa_2Cu_3O_{7-\delta}$ samples (YBCO), c_V has a critical behavior that is well represented by the three-dimensional (3D) XY model. In a magnetic field, the singularity is washed out and the maximum again moves to lower temperatures. For $Bi_2Sr_2CaCu_2O_{8+\delta}$ samples (BSCCO) on the other hand, c_V is rather symmetric around the critical temperature.[1] Besides a possible singular behavior very close to T_c, it resembles the specific-heat curve of a system of noninteracting bosons in 3D that undergo a Bose-Einstein condensation (BEC). In a magnetic field, the maximum of the curve loses its height, but the position of the maximum remains at the zero-field critical temperature, rather than to follow the field-dependent T_c. This is again a characteristic feature of BEC.[2]

(2) The one-electron spectral functions have been studied by photoemission[3] and tunneling[4] experiments. They have revealed that underdoped cuprates develop a pseudogap in the electronic spectrum, and thus in the electronic density of states, well above the transition temperature T_c. When T increases above T_c, this pseudogap is gradually filled, but its width only weakly depends on temperature. The pseudogap essentially disappears at some temperature T^* that increases when one goes towards the underdoped limit. The **k** dependence of the pseudogap is the same as for the superconducting gap existing below T_c. Other experimental observations, such as the anomalous T dependence of the Pauli susceptibility or of the nuclear magnetic resonance relaxation time are likely to be linked to the occurrence of the pseudogap, but we will not discuss them here.[5]

The microscopic origin of this pseudogap is at present a controversial subject. The fact that it has the same angular dependence as the superconducting gap and thus goes over smoothly into the latter when T_c is crossed, respectively "coexists" with it below T_c, has found diverging interpretations. It has been taken as a demonstration of strong superconducting, respectively pairing fluctuations above T_c,[6] whereas other authors conclude, from the different B dependences of superconducting and pseudogap, that the latter is not directly related to the phenomenon of superconductivity.[7] It has also been pointed out that the usual temperature T^*, that joins T_c somewhere near optimal doping, is actually not well defined, and that a more systematic characteristic temperature, related to the width of the pseudogap, points to the existence of a (hidden) quantum phase transition.[8]

A current interpretation of these facts is based on the idea[9] of a crossover from a more BCS-like superconductivity for optimally and overdoped samples, where pairing and condensation occur essentially at the same temperature, to a superconductivity produced by preformed pairs of electrons, that are formed around T^*, well above T_c, whereas the phase coherence necessary for the collective behavior of the superconductor is only established at a lower temperature T_c. This view is consistent with the fact that the low-temperature coherence length is much shorter in the underdoped regime, a fact that supports the picture of pairs that are well localized in space. Moreover, underdoped materials

typically get more and more anisotropic when the doping is decreased, such that the effective mass of these preformed pairs is much larger in the crystallographic c direction than in the a-b plane. The formation of a pseudogap induced by pair fluctuations is probably also favored by a low spatial dimensionality.

In the absence of a full understanding of the microscopic mechanism that produces high-temperature superconductivity, the attractive Hubbard model[10] is a useful and relatively simple tool in order to describe various properties of a superconductor. In particular, the crossover between weak coupling (long coherence length) and strong coupling (short coherence length) regimes can easily be achieved by varying the strength of the attraction.[11] In this context it is useful to stress that the concept of coherence length is associated here with the spatial extension of the Cooper pairs, not to be confounded with the phase correlation length describing the distance over which pairing fluctuations are correlated, which is a nonmonotonic function of the coupling strength at $T=0$.[12] Most often the simple case of a local attraction between electrons of opposite spin sitting on the same lattice site and leading to s-wave pairing has been considered, but in order to take into account nontrivial order parameter symmetries, extensions including nearest-neighbor attraction have also been treated.[13] Insight into the properties of this model in two spatial dimensions has been obtained by various analytical approximations, such as functional integral techniques,[14] the self-consistent T matrix,[15] the fluctuation exchange (FLEX)[16] or the Hubbard-alloy-analogy approach,[17] and by quantum Monte Carlo (QMC) simulations.[18]

Analytic work usually aims at describing the main effect of the attractive interaction by a coupling between one-electron quantities and the two-particle propagator that manifests the tendency toward the formation of pairs. In the T-matrix approach, some details of which will be recalled in Sec. II, this is manifest in the explicit form of the electronic self-energy. Decoupling of the interaction by a Stratonovich-Hubbard transformation allows to represent the free energy of the system in terms of a classical pairing field. For weak interaction the action governing this field is of the Landau-Ginzburg type, whereas for strong interaction it has the Gross-Pitaevski form, describing interacting preformed bosonic pairs.[14,19] In this regime the corresponding one-electron spectral function shows two bands,[18,20] one with states for unpaired electrons and the other with pair states, separated by a "correlation gap." The crossover region between the two regimes is more complicated. In particular, a perturbative approach is delicate in the regime where the effective chemical potential moves out of the noninteracting band.[21]

Numerical work[18] has yielded interesting information about thermodynamic properties, such as the temperature dependence of the chemical potential or the spin susceptibility. Moreover, it has revealed the occurrence of a pseudogap centered around the chemical potential that arises for intermediate values of the coupling and develops into a band splitting when the coupling gets stronger.

In the present paper, we treat the T-matrix equations for intermediate values of the coupling U, i.e., for attraction energy of a local pair on the order of half of the noninteracting bandwidth W. In this case, the chemical potential μ of the interacting system is still inside the noninteracting band, contrary to the strong-coupling regime, where U is typically larger than W and μ is below the noninteracting band, leading to the "correlation gap" mentioned above. We solve the equations by simple analytical calculations that guarantee a minimal approximate self-consistency between the one-electron propagator and the T matrix, describing pair excitations. In order to relate the spectral properties of the renormalized electrons to the thermodynamics of the system, we also evaluate the grand canonical potential in the same T-matrix approximation.[22] Since we do not solve the T-matrix equations numerically in their full self-consistency, we will take over some results from QMC in 2D for our calculations.[18] Our main goal is to show that in the temperature regime where the electronic pseudogap is almost fully developed, with a width that is larger than $k_B T_c$, the thermodynamic properties of the system can, to a good approximation, be described by unpaired electrons and weakly interacting and long-living preformed pairs.[23] The latter obey Bose statistics and their chemical potential shows the tendency to vanish when the critical temperature T_c is approached from above. Thus the BEC scenario for the superconducting phase transition seems to be suited not only for the case where the coupling is "literally" strong—typically larger than the noninteracting bandwidth, which seems relatively unrealistic for real materials—but also for the low-density intermediate coupling regime, provided that the system develops a pseudogap with a sufficient width. Since we are interested in applying our considerations to underdoped high-temperature superconductors, we include a weak coupling between the lattice planes which, if it is small enough, preserves for the 3D case the conclusions drawn in 2D about the BEC scenario. Moreover, due to the special nature of the superconducting phase transition in a strictly 2D system (Berezinskii-Kosterlitz-Thouless vortex unbinding transition) that cannot be addressed by the T-matrix approach,[24] the extension to a 3D (anisotropic) system is essential in guaranteeing the validity of the latter method, since we deal then with an "ordinary" bulk phase transition. The question then arises to know whether the bosons described by the T matrix are able to characterize completely this phase transition. The value of the critical temperature shows that the unpaired electrons cannot be omitted in this context, although their contribution to the thermodynamic potential is featureless at $T=T_c$. We finally discuss some implications of these considerations for the thermodynamic properties of underdoped cuprates.

In Sec. II we recall the basic equations for the one- and two-electron propagators, as well as the grand canonical potential, in the T-matrix approximation. In Sec. III, we present our strategy that consists in a perturbative calculation of the electronic self-energy, an approximate calculation of the parameters determining the T matrix, based on a simple analytic form of the pseudogap structure, and a suitable expansion of the grand canonical free energy. Concrete results are presented in Sec. IV, where we also use some "cross-checks" in order to confirm the validity of our simple proce-

dure. We analyze then the applicability of the BEC scenario. The text ends with a summary in Sec. V. Various more technical parts of the calculations are presented in Appendices A–D.

II. THEORETICAL FRAMEWORK OF THE *T*-MATRIX APPROXIMATION

We start from the Hubbard model with a local attraction ($-U$, with $U > 0$) and a nearest-neighbor hopping $t > 0$ defined on a 2D square lattice:

$$\mathcal{H} = -t \sum_{\langle i,j \rangle, \sigma = \uparrow, \downarrow} (c_{i\sigma}^{\dagger} c_{j\sigma} + \text{H.c.}) - U \sum_i n_{i\downarrow} n_{i\uparrow}$$

$$- \mu \sum_i (n_{i\downarrow} + n_{i\uparrow}) \qquad (1)$$

with creation (annihilation) operators $c_{i\sigma}^{\dagger}$ ($c_{i\sigma}$) for an electron of spin σ on lattice site i, and $n_{i,\sigma} = c_{i\sigma}^{\dagger} c_{i\sigma}$ being the corresponding density. In the well-known self-consistent *T*-matrix approach,[25] which is the ladder approximation to the Bethe-Salpeter equation,[26] the electronic self-energy $\sigma(\mathbf{k}, z_\nu)$ describes scattering of electronic quasiparticles from pairing fluctuations. The latter are described by the *T* matrix that takes into account repeated two-particle scattering processes:

$$T^{-1}(\mathbf{k}, z_\alpha) = \frac{1}{U} - \chi(\mathbf{k}, z_\alpha), \qquad (2)$$

$$\chi(\mathbf{k}, z_\alpha) = \frac{1}{\beta N} \sum_{\mathbf{q}, z_\nu} G(\mathbf{k} - \mathbf{q}, z_\alpha - z_\nu) G(\mathbf{q}, z_\nu), \qquad (3)$$

$$G^{-1}(\mathbf{k}, z_\nu) = G_0^{-1}(\mathbf{k}, z_\nu) - \sigma(\mathbf{k}, z_\nu), \qquad (4)$$

$$\sigma(\mathbf{k}, z_\nu) = -\frac{1}{\beta N} \sum_{\mathbf{q}, z_\alpha} G(\mathbf{k} - \mathbf{q}, z_\alpha - z_\nu) T(\mathbf{q}, z_\alpha). \qquad (5)$$

Here β is the inverse temperature T^{-1} (we take $\hbar = k_B = 1$ from now on), N the number of lattice sites, the $\mathbf{q}$ sums run over a 2D Brillouin zone $[-\pi, \pi] \times [-\pi, \pi]$ (wave vectors are in units of the inverse lattice constant) and z_ν and z_α are fermionic and bosonic Matsubara frequencies, respectively. The quantity G is the one-electron Green function and is related by Dyson's equation (4) to its noninteracting form given by

$$G_0(\mathbf{k}, z_\nu) = \frac{1}{z_\nu - \xi_{\mathbf{k}}}, \qquad (6)$$

where $\xi_{\mathbf{k}} = \varepsilon_{\mathbf{k}} - \mu$ contains the dispersion associated to the Hamiltonian (1). As for $\varepsilon_{\mathbf{k}}$, the zero of the chemical potential μ is the middle of the *noninteracting* band, so that $\mu = -U/2$ corresponds to a half-filled band for any U or T. The value of the noninteracting bandwidth W is equal to $8t$ for the two-dimensional tight-binding case considered here.

The *T*-matrix approach has been used by many authors[10,15,20] in order to describe various properties of the model (1) for low electronic densities where the neglect of

more complicated scattering processes should be justified. The same set of equations can be obtained in leading order in $1/M$ for a generalized Hubbard model in which the electronic operators have M "colors." [27] The corresponding approximation for the grand canonical potential Ω can be expressed by the same quantities,[22]

$$\Omega(T, V, \mu) = -\frac{2}{\beta} \text{Tr}[\sigma G + \ln(\sigma - G_0^{-1})] + \Phi[G]. \qquad (7)$$

Here the symbol Tr means summation over wave vectors and Matsubara frequencies, and the functional Φ is given by

$$\Phi[G] = \frac{1}{\beta} \text{Tr}[\ln(T^{-1})] \qquad (8)$$

such that the self-energy can formally be obtained by a functional derivative,

$$\sigma = \frac{1}{2} \frac{\delta \Phi[G]}{\delta G}. \qquad (9)$$

Such a form for Ω has been used for the same model in Ref. 21 with a more general form for $\Phi[G]$.

A self-consistent solution of the above equations can only be achieved numerically. Our aim is to evaluate G and Ω analytically by approximating $T(\mathbf{k}, z_\alpha)$ and the one-electron spectral functions by simple forms that will partly be based on results obtained by numerical work in the framework of the *T*-matrix approach[10,15,20,28,29] and by quantum Monte Carlo simulations.[18] While the main part of our calculations will be done for a 2D realization of the model (1), i.e., for a single lattice plane of the superconductor, we will indicate at the end how a weak coupling between planes would modify the results. The different steps of our calculation are presented in the following section and corresponding concrete results for $U = 4t$ are given in Sec. IV.

III. APPROXIMATE SELF-CONSISTENT CALCULATION

A. Analytic form of the *T* matrix

We consider an intermediate interaction strength $U = 4t$. From numerical *T*-matrix calculations,[15,30] we borrow the fact that for U values that are at least as large as half the noninteracting bandwidth, the imaginary part of $T(\mathbf{k}, z_\alpha \to \omega + i\eta)$ develops a pronounced peak located around a single energy value ω [in the weak-coupling limit Im(T) has, at least for small wave numbers k, a resonance form that is antisymmetric with respect to $\omega = 0$, like the spectral function of a harmonic phonon]. Thus, T can be associated with the propagator of a bosonic quasiparticle, a virtual pairing state of two electrons. We approximate this propagator by the following simple low-energy and small-wave-number form,

$$T^{-1}(\mathbf{k}, z_\alpha) \approx a + ck^2 - dz_\alpha, \qquad (10)$$

in which the detailed dispersion is replaced by an isotropic parabolic wave-vector dependence (in an effective Brillouin zone of spherical symmetry). The coefficients involved in Eq. (10) are related to the particle-particle bubble χ in expression (3) by

$$a = \frac{1}{U} - \chi(0,0), \tag{11}$$

$$c = -\frac{1}{2} \frac{\partial^2}{\partial k^2} \chi(\mathbf{k},0)|_{k=0}, \tag{12}$$

$$d = \frac{\partial}{\partial \omega} \chi(0, z_\alpha = \omega + i\eta)|_{\eta \to 0, \omega = 0}. \tag{13}$$

The coefficient d is in general complex and, correspondingly, the virtual pairs described by Eq. (10) have a finite lifetime. According to the Thouless criterion,[31] the transition to a superconducting state takes place when $T(0,0)$ diverges, i.e., when the "chemical potential" proportional to a of the quasiparticle described by Eq. (10) becomes zero. This is a reasonable criterion in three dimensions, but in a strictly 2D system the corresponding phase transition is expected to be of the Berezinskii-Kosterlitz-Thouless (BKT) type: there is no true long-range order at any finite temperature but the superconducting coherence is manifested by a finite helicity modulus (or phase stiffness) below the transition temperature T_{BKT}. This quantity is associated with the nontrivial response of the system to a phase twist imposed from outside and appears even in the absence of a finite order parameter, unlike in a "normal" second-order transition where the latter is the fundamental characteristics of the ordered state below T_c. Deisz and Serene[32] have realized such a 2D scenario in the framework of a FLEX calculation, the essential element of which corresponds to the T-matrix approximation. They have found that $T^{-1}(0,0)$ as a function of the temperature T effectively tends to zero for $T \searrow T_{BKT}$, but bends at $T = T_{BKT}$ and finally reaches zero only at $T = 0$. Here we are mainly interested in the behavior of the system above the critical temperature. Moreover, the following strictly 2D calculations will finally be generalized in order to include a weak interplane coupling, as it is expected for strongly anisotropic materials such as BSCCO. Thus we will take a coefficient a that tends to zero as a sign of an incipient phase transition, as it would be appropriate for three dimensions.

B. One-electron Green function

The electronic self-energy (5) can now be approximated using the simple form (10) for T and replacing G by the noninteracting limit G_0:

$$\sigma(\mathbf{k}, z_\nu) \approx \sigma_0(\mathbf{k}, z_\nu) = -\frac{1}{\beta N} \sum_{\mathbf{q}, z_\alpha} G_0(\mathbf{k} - \mathbf{q}, z_\alpha - z_\nu) T(\mathbf{q}, z_\alpha). \tag{14}$$

This expression has been evaluated by Capezzali and Beck[28] for an isotropic system by choosing values for the coefficients a, c, and d that are compatible with self-consistent T-matrix calculations.[15] The resulting imaginary part of σ has a relatively sharp peak.[28] When $\mathbf{k}$ crosses the Fermi wave number, the peak position of $\text{Im}(\sigma_0)$ moves in the opposite direction with respect to the peak of the noninteracting electronic energy. The corresponding one-electron band thus develops a pseudogap centered around the Fermi energy. Its

depth increases when a becomes smaller and it is fully developed when $a = 0$. A simple estimate for the width of the pseudogap can be obtained by concentrating the total weight of the pair fluctuations in the sum (14) over $\mathbf{q}$ and z_α on the values $q = z_\alpha = 0$ (the total bandwidth of the pair fluctuations, represented by $T(\mathbf{q}, z_\alpha)$, is indeed smaller than the free electron bandwidth, see Sec. IV). The resulting simplified self-energy has BCS-like form,

$$\sigma_0(\mathbf{k}, z_\nu) \approx \frac{\Delta_0^2}{z_\nu + \xi_{\mathbf{k}} + i\Gamma_0} \tag{15}$$

with

$$\Delta_0^2 = \frac{1}{\beta N} \sum_{\mathbf{q}, z_\alpha} T(\mathbf{q}, z_\alpha). \tag{16}$$

The effect of the full summation over $\mathbf{q}$ and z_α in Eq. (14) has been simulated by introducing a finite lifetime Γ_0 into the Green function. The result (15) indeed reproduces quite well the form of σ_0 found numerically.[28] The half-width of the pseudogap is then approximately given by

$$\Delta = \sqrt{\Delta_0^2 - (\Gamma_0/2)^2}. \tag{17}$$

C. Approximate self-consistent evaluation of the T-matrix coefficients

As a next step on the way to a self-consistent solution of our basic equations (2)–(5), the parameters determining the T-matrix should now be (re-)calculated according to equations (2) and (3), by inserting into χ the one-electron Green function G with the self-energy found in Sec. III B. For our purposes, it will be sufficient to know the features of the corresponding spectral functions A. As obtained by numerical calculations,[28] the latter have essentially a BCS form with two branches around the chemical potential, but with a finite linewidth. Therefore, we will use the following method to evaluate the coefficients a, c, and d of the T matrix. First we reexpress the latter in terms of the BCS electronic spectral function that is given by

$$A_{BCS}(\mathbf{k}, \omega) = 2\pi [u_{\mathbf{k}}^2 \delta(E_{\mathbf{k}} - \omega) + v_{\mathbf{k}}^2 \delta(E_{\mathbf{k}} + \omega)], \tag{18}$$

with

$$E_{\mathbf{k}} = \sqrt{\Delta^2 + \xi_{\mathbf{k}}^2}, \tag{19}$$

$$u_{\mathbf{k}}^2 = \frac{1}{2}\left(1 + \frac{\xi_{\mathbf{k}}}{E_{\mathbf{k}}}\right), \tag{20}$$

$$v_{\mathbf{k}}^2 = \frac{1}{2}\left(1 - \frac{\xi_{\mathbf{k}}}{E_{\mathbf{k}}}\right). \tag{21}$$

This is explained in Appendix A. The full results, shown in Appendix B, are expressed as energy integrals involving the BCS density of states combined with appropriate weight factors, as it has been done for deriving the Ginzburg-Landau theory below T_c.[33] In a somewhat simplified form, they read

$$a = \frac{1}{U} - \int d\omega D_{a,1}(\omega) \frac{\tanh(\beta\omega/2)}{2\omega}, \qquad (22)$$

$$
\begin{aligned}
c = \int d\omega \Bigg\{ & D_{c,11}(\omega) \frac{\tanh(\beta\omega/2)}{2\omega} \\
& + D_{c,31}(\omega) \Bigg[\frac{\tanh(\beta\omega/2)}{4\omega^2} + \frac{n_F'(\omega)}{2\omega} \Bigg] \\
& + D_{c,51}(\omega) \Bigg[-\frac{\tanh(\beta\omega/2)}{4\omega^3} - \frac{n_F'(\omega)}{2\omega^2} + \frac{n_F''(\omega)}{2\omega} \Bigg] \Bigg\} \\
& \times \frac{1}{2} \left(\frac{d\xi_{\mathbf{k}}}{dk} \right)^2_{k=k_F} \\
& + \int d\omega D_{c,32}(\omega) \Bigg[\frac{\tanh(\beta\omega/2)}{4\omega^2} + \frac{n_F'(\omega)}{2\omega} \Bigg] \left(\frac{d^2\xi_{\mathbf{k}}}{dk^2} \right)_{k=k_F},
\end{aligned}
$$
$$(23)$$

$$d = \mathcal{P} \int d\omega D_{a,1}(\omega) \frac{\tanh(\beta\omega/2)}{4\omega^2} + i\frac{\pi}{8}\beta D_{a,1}(\omega=0), \qquad (24)$$

where $\mathcal{P}$ denotes the Cauchy principal part. The integrals over energy involve various effective densities of states obtained by summing over particular weights and given in details in Appendix B. They are all based on the BCS density of states

$$
D_{\mathrm{BCS}}(\omega) = \begin{cases} D_0[\mu_0 + \xi(\omega)] \dfrac{|\omega|}{\sqrt{\omega^2 - \Delta^2}}, & |\omega| \geq \Delta \\[2ex] 0, & |\omega| < \Delta, \end{cases} \qquad (25)
$$

where $\xi(\omega) = \mathrm{sgn}(\omega)\sqrt{\omega^2 - \Delta^2}$ and D_0 is the density of states for the 2D tight-binding model given by Eq. (A10) and corresponding to the kinetic energy of the Hamiltonian (1). The quantity μ_0 gives the position of the pseudogap inside the interacting band (the Fermi energy) and has to satisfy the usual condition of fixing the density n. In the particular case of a BCS-like electronic structure, it takes a very simple form:

$$n \equiv \int d\epsilon D_{\mathrm{BCS}}(\epsilon - \mu_0)\theta(\mu_0 - \epsilon) = \int d\epsilon D_0(\epsilon)\theta(\mu_0 - \epsilon), \qquad (26)$$

where θ is the Heaviside step function. Therefore, μ_0 corresponds to the (zero-temperature) chemical potential of non-interacting electrons having the same density n. However, in the present context where $U \neq 0$, μ_0 does not provide the value of the "true" chemical potential μ because it is defined with respect to the middle of the *interacting* band whose location is not specified (whereas μ is measured with respect to the middle of the *noninteracting* band and will be given later in Sec. IV A). We also remark that the limit $\Delta \to 0$ in Eqs. (22)–(24) is well defined and gives the usual expressions found in the literature.[14]

The finite width of the spectral functions in the pseudogap (PG) regime is now taken into account by replacing the δ functions in Eq. (18) by a normalized distribution function f_Γ with a finite width Γ,

$$A_{\mathrm{PG}}(\mathbf{k}, \omega) = 2\pi[u_{\mathbf{k}}^2 f_\Gamma(E_k - \omega) + v_{\mathbf{k}}^2 f_\Gamma(E_{\mathbf{k}} + \omega)], \qquad (27)$$

that involves the same quantities $E_{\mathbf{k}}$, $u_{\mathbf{k}}$, and $v_{\mathbf{k}}$ as before. In reality, the spectral width Γ depends on wave number and temperature: it is the largest near the Fermi wave number k_F where the pseudogap is created and increases with temperature.[28] In order to deal with simple expressions, we choose a line shape that is the same for all $\mathbf{k}$ at T_c and that eventually develops a peak around k_F when one goes away from the transition. A useful choice of the distribution function is

$$f_\Gamma(\omega) = \frac{1}{\sqrt{2\pi}\Gamma} \exp\left[-\frac{1}{2}\left(\frac{\omega}{\Gamma}\right)^2 \right]. \qquad (28)$$

Using these "broadened BCS spectral functions," we can evaluate the coefficients a, c, and d. As shown in Appendix C, their expressions keep the form (22)–(24), but all the corresponding "densities of states" (B4)–(B10) have to be systematically replaced by expressions taking into account the finite width of the spectral function (27). For instance, D_{BCS} from Eq. (25) becomes

$$D_{\mathrm{PG}}(\omega) = \int dE D_{\mathrm{BCS}}(E) f_\Gamma(E - \omega). \qquad (29)$$

This expression shows clearly how the BCS density of states is modified by the finite linewidth $\Gamma > 0$, which displaces an increasing amount of spectral weight inside the gap region $[-\Delta, \Delta]$ when the temperature T becomes larger so that the pseudogap gets gradually "filled."

D. Expansion of the grand canonical potential

In the general expression (7) for the grand canonical potential only the third term, given by Eq. (8), has an immediate interpretation: it has the form of the free energy of non-interacting bosonic pair fluctuations, represented by the T matrix. Indeed, when the imaginary part of the coefficient d is small, expression (10) is the propagator of bosonic quasi-particles with chemical potential $\mu_B = -a/\mathrm{Re}(d)$ and weight $Z_B = 1/\mathrm{Re}(d)$. The first two terms of Ω in Eq. (7) can be given a more concrete meaning by expanding G in powers of the self-energy σ and using the explicit form (5) for the latter. To second order in σ, we are left with two terms beside $\Phi[G]$ so that Ω reads

$$\Omega \approx \Omega_0 + \Omega_b + \Omega_i, \qquad (30)$$

where

$$\Omega_0 = -\frac{2}{\beta} \sum_{\mathbf{k}, z_\nu} \ln[-G_0(\mathbf{k}, z_\nu)^{-1}], \qquad (31)$$

$$\Omega_b = \frac{1}{\beta} \sum_{\mathbf{k}, z_\alpha} \ln[T(\mathbf{k}, z_\alpha)^{-1}], \qquad (32)$$

$$\Omega_i = -\frac{1}{\beta} \sum_{\mathbf{k}, z_\nu} G_0^2(\mathbf{k}, z_\nu) \sigma^2(\mathbf{k}, z_\nu). \tag{33}$$

Here Ω_0 is the free energy of noninteracting particles that do not participate in the pairing fluctuations. They have the unperturbed tight-binding spectrum of the Hamiltonian (1), but they are subject to the "true" chemical potential μ that yields the correct number of electrons in the presence of the attraction. Ω_b is the bosonic contribution, as mentioned above. The last contribution Ω_i describes an interaction between the bosonic excitations. It can be given a more transparent form after replacing $\sigma(\mathbf{k}, z_\nu)$ by its explicit expression (5),

$$\Omega_i = -\frac{1}{\beta} \sum_{\mathbf{k}, z_\alpha} T(\mathbf{k}, z_\alpha) \sigma_b(\mathbf{k}, z_\alpha), \tag{34}$$

where σ_b represents a bosonic self-energy defined as

$$\sigma_b(\mathbf{k}, z_\alpha) = \frac{1}{\beta N} \sum_{\mathbf{q}, z_\beta} T(\mathbf{q}, z_\beta) R(\mathbf{k}, \mathbf{q}, z_\alpha, z_\beta), \tag{35}$$

$$R(\mathbf{k}, \mathbf{q}, z_\alpha, z_\beta) = \frac{1}{\beta N} \sum_{\mathbf{p}, z_\nu} G(\mathbf{k} - \mathbf{p}, z_\alpha - z_\nu)$$
$$\times G(\mathbf{q} - \mathbf{p}, z_\beta - z_\nu) G_0^2(\mathbf{p}, z_\nu). \tag{36}$$

The above equations show that Ω_i is exactly the Hartree-Fock term of the free energy of bosons interacting through the potential R.[26] "Bare" bosons are described by the T matrix, whereas the propagator of the corresponding "dressed" quasiparticles satisfies Dyson's equation,

$$T_d^{-1}(\mathbf{k}, z_\alpha) = T^{-1}(\mathbf{k}, z_\alpha) - \sigma_b(\mathbf{k}, z_\alpha). \tag{37}$$

It is then possible to write the bosonic part of the free energy in a simpler way,

$$\Omega_b + \Omega_i = \Omega_d = \frac{1}{\beta} \sum_{\mathbf{k}, z_\alpha} \ln[T_d^{-1}(\mathbf{k}, z_\alpha)]. \tag{38}$$

The main effect of the bosonic interaction is thus a renormalization of the T-matrix coefficients a, c, and d and will be discussed in the next section. For the moment, we consider the equation for the particle number that determines the chemical potential μ by imposing a given density of particles n per site,

$$n \equiv \frac{1}{N} \sum_i \langle n_{i\uparrow} + n_{i\downarrow} \rangle = -\frac{1}{N} \frac{\partial \Omega}{\partial \mu}, \tag{39}$$

where N is the number of lattice sites. Starting from Eq. (7) for Ω and using the relations (2)–(5) that determine the T matrix, it is easy to show that Eq. (39) reduces to

$$n = \frac{2}{\beta N} \sum_{\mathbf{k}, z_\nu} G(\mathbf{k}, z_\nu), \tag{40}$$

which is obviously correct, but formal, in the sense that it does not distinguish between unpaired-electron and bosonic contributions to the total particle number. In order to intro-

duce this "two-fluid concept" into the number equation (39), we can use the decompositions (30) and (38) for Ω. This yields a particularly transparent result if $\mathrm{Im}(d)$ can be neglected as shown later (Sec. IV A 2),

$$n = n_0 + n_d. \tag{41}$$

The first term represents the unpaired electrons, the number of which is given by

$$n_0 = \frac{2}{N} \sum_{\mathbf{k}} n_F(\varepsilon_{\mathbf{k}} - \mu), \tag{42}$$

where n_F is the Fermi-Dirac distribution and μ is the "true" chemical potential, not to be confounded with μ_0 defined previously in the framework of our model for the electronic structure. The second term reads

$$n_d = \frac{1}{\beta N} \sum_{\mathbf{k}, z_\alpha} T_d(\mathbf{k}, z_\alpha) \frac{\partial}{\partial \mu} T_d^{-1}(\mathbf{k}, z_\alpha) \tag{43}$$

and gives the number density of electrons involved in the pairing fluctuations. As explained above, the latter can be described in terms of interacting bosons and will be discussed more extensively below.

We finally stress that the expressions (31)–(33) do not represent the only possible decomposition of the free energy. In fact one could imagine finding other approximate forms of Ω that would, for example, also introduce effective interactions between the unpaired electrons or between unpaired electrons and pairs. However, as it has just been shown, they are well suited to study the thermodynamic properties of the system and to find the nature of the degrees of freedom that are dominating in the pseudogap regime just above T_c.

E. Effects of the bosonic interaction

The previous section has introduced an interaction between the bosonic quasiparticles that was formulated by the Hartree-Fock approximation to the self-energy given by Eq. (35). In order to get some insight into the effects of this interaction, we first calculate the Hartree contribution to the grand canonical potential that is essentially given by expression (36) evaluated at zero arguments. We obtain

$$\Omega_{i,\text{Hartree}} = -Nb \left[\frac{1}{\beta N} \sum_{\mathbf{k}, z_\alpha} T(\mathbf{k}, z_\alpha) \right]^2, \tag{44}$$

where we have introduced the coefficient b defined by

$$b = \frac{1}{\beta N} \sum_{\mathbf{k}, z_\nu} G^2(\mathbf{k}, -z_\nu) G_0^2(\mathbf{k}, z_\nu) \tag{45}$$

and that will be discussed below. Expression (44) corresponds exactly to the result that would be obtained by performing a variational calculation for the free energy of the time-dependent Landau-Ginzburg theory based on Bogoliubov's inequality. An even deeper analogy can be found by considering the instantaneous approximation of the interaction potential (36), i.e., by setting both frequencies z_α and z_β to zero. In this case our approach is structurally identical to a

perturbative treatment of the Gross-Pitaevski equation[34] that is used to describe the physics of interacting bosons. Therefore, we can base ourselves on known results about the latter problem in order to determine the effects of the interaction R.

First, coming back to the coefficient b defined above, we anticipate the fact that it becomes small for an electronic structure containing a well-developed pseudogap, as it will be discussed in more details in the next section. In this case we expect only small changes induced by the interaction which then manifests itself essentially by a weak renormalization of the T-matrix parameters a, c, and d. This could be calculated in principle by performing a low-energy expansion of $R(\mathbf{k},\mathbf{q},z_\alpha,z_\beta)$, in the same way as it has been done for $T^{-1}(\mathbf{k},z_\alpha)$ in Eq. (10). However, due to the already approximative nature of our treatment, it is not sure that the obtained results would still be meaningful. We thus do not undertake such a calculation and will subsequently neglect the effects of the interaction on the T-matrix coefficients,

$$T_d(\mathbf{k},z_\alpha) \approx T(\mathbf{k},z_\alpha). \tag{46}$$

We are now able to calculate explicitly the bosonic density by reconsidering Eq. (43). Performing the frequency summation and assuming that a contains the only relevant dependence in μ, we find

$$n_d \approx \frac{1}{N} \sum_{\mathbf{k}} n_B(\Omega_{\mathbf{k}}) \left(-\frac{\partial \Omega_{\mathbf{k}}}{\partial \mu} \right). \tag{47}$$

This expression involves the Bose-Einstein distribution n_B for particles having the dispersion

$$\Omega_{\mathbf{k}} = \frac{1}{\mathrm{Re}(d)} (a + ck^2), \tag{48}$$

Im(d) being neglected. The usual $\mathbf{k}$ sum is weighted by a factor that will be evaluated below. These relations together with Eq. (41) show that the total number of particles splits into the number of free plus the number of paired electrons, in agreement with the "two-fluid" idea underlying our approach. This is, however, not true anymore when the pseudogap fills up, because then both the interaction and the imaginary part of the coefficient d cannot be neglected.

IV. RESULTS

A. T-matrix coefficients

The coefficients a, c, d, and b can now be calculated for the pseudogap regime of the attractive Hubbard model (1) by evaluating the corresponding expressions exhibited in Sec. III. The result depends on various parameters for which we have to choose appropriate values. Our objective is to describe the behavior of the model for a low density of charge carriers, for which the T-matrix approach should be relevant. We take

$$n = 0.2 \tag{49}$$

in a normalization where, in agreement with Eq. (40), $n = 2$ corresponds to a filled band. Given this condition, we fix the relevant parameters as follows:
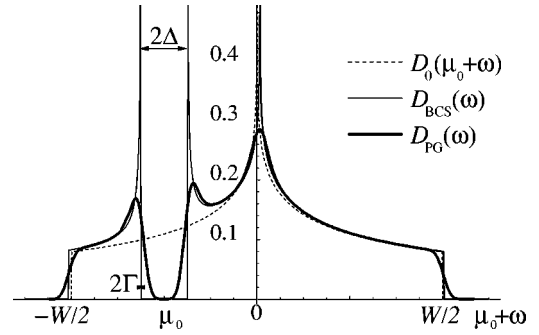

FIG. 1. Shapes of the density-of-state function for various cases: $\Delta = \Gamma = 0$ ("weak coupling"), $\Delta > 0$, $\Gamma = 0$ ("BCS") and Δ, $\Gamma > 0$ ("pseudogap"). The chosen parameter values are $\Delta = 0.5t$ and $\Gamma = 0.125t$ (see Sec. IV A).

(1) We consider temperatures in the interval $[T_c, T^*]$ that corresponds to the region where the pseudogap is first fully developed and then gradually fills up. This qualitative behavior is borrowed directly from QMC results.[18] The corresponding temperature values are deduced from other works[22,35] that consider the limit of infinite system size. They provide the estimates $T_c \approx 0.07t$ and $T^* \approx 0.2t$. We also mention that, by assuming a bandwidth $W = 8t \sim 1$ eV, the corresponding critical temperature would be of the order of 50 K, which makes sense for underdoped high-temperature superconductors.

(2) The width of the pseudogap, which is essentially given by 2Δ, can also be estimated from QMC calculations.[18] For a U value of the order of half the bandwidth, i.e., $U = 4t$, this quantity is of the order of t. Thus we choose $\Delta = 0.5t$.

(3) As stated above, the width of the electronic spectral function depends on the electronic wave number k and on the temperature T.[28] However, for temperatures just above T_c it is sufficient to take a constant value and we thus choose

$$\Gamma = 0.125t. \tag{50}$$

This yields appropriate values of the spectral width around the Fermi wave number where the main contribution to the coefficients a, c, and d comes from. This choice of Δ and Γ yields the one-electron density of states $D_{PG}(\omega)$ shown in Fig. 1. For higher temperatures, we must take into account the dependences of Γ in both T and $\mathbf{k}$ in order to reproduce the "filling" of the pseudogap.[28] This is done by adding to Γ a $\mathbf{k}$-dependent contribution centered around the Fermi wave vector and becoming larger as the temperature increases. This mechanism, which is not relevant to the subsequent calculations that are restricted to temperatures close to T_c, is illustrated in Fig. 2.

(4) Solving Eq. (26) for $n = 0.2$ gives the result $\mu_0 = -2.9t$, which is only weakly temperature dependent for $T < T^*$, as observed by replacing $\theta(\mu_0 - \epsilon)$ by $n_F(\epsilon - \mu_0)$ in Eq. (26). This value must be compared with the corresponding QMC data[18] where the "true" chemical potential
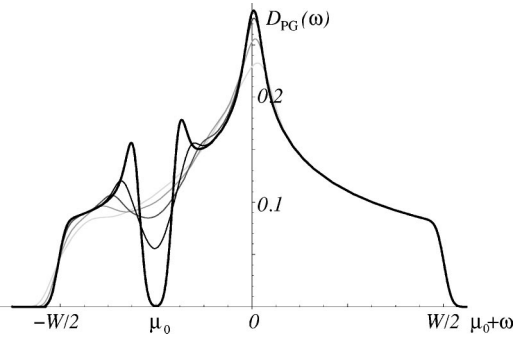
FIG. 2. Filling of the pseudogap with increasing temperature by varying the linewidth Γ. The thickest curve is obtained for $\Gamma = 0.125t$ ($T = T_c$). The thin curves require the additional **k**-dependent contribution to Γ mentioned in the text. For the highest temperature (lightest curve), it is characterized by a maximal height of 8Γ and a width of 3Δ around $\xi_{\mathbf{k}} = 0$.

μ is calculated for the same density $n = 0.2$. Since the latter is measured with respect to the middle of the noninteracting band, it fixes the "absolute" position of the interacting band (inside which μ_0 gives the position of the pseudogap). One finds $\mu = -3.5t$ for the same values of U and n as used here. Therefore, the interacting band is shifted to lower energies by a small amount,

$$\mu - \mu_0 = -0.6t. \tag{51}$$

This feature, illustrated in Fig. 3 and in agreement with other studies,[15,36] will be used in Sec. IV B in connection with the number equation (41).

Given these parameter values, we obtain the results given in Table I and commented hereafter.

1. Coefficient a

Its dependence on the temperature T is shown in Fig. 4 together with the weak-coupling case.[14] Two facts are important. First, when the pseudogap is wider than T and its depth reaches its maximum value, as it is the case for $T \searrow T_c$, the
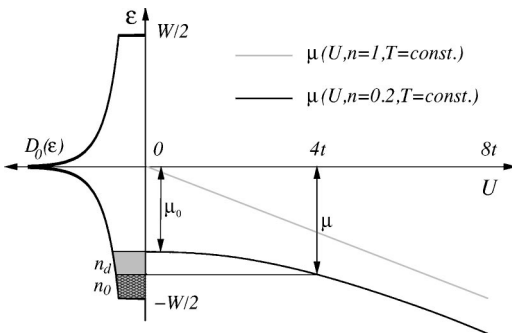

FIG. 3. Schematic behavior of the chemical potential μ when varying the interaction strength U. At half-filling ($n = 1$), it is always equal to $-U/2$. For small densities ($n \sim 0.2$), it reaches this value only asymptotically in the strong-coupling regime. At intermediate coupling ($U = 4t$), the difference $\mu - \mu_0$ allows to visualize the two contributions to the electronic density n discussed in the text.

TABLE I. T-matrix coefficients for various cases ($\beta = T_c^{-1} = 15t^{-1}$ and $n = 0.2$).

Coefficient	Weak coupling $\Delta = \Gamma = 0$	BCS $\Delta = 0.5t,\ \Gamma = 0$	Pseudogap $\Delta = 0.5t,\ \Gamma = 0.125t$
$a[t^{-1}]$	0.158	0.019	0.021
$c[t^{-1}]$	2.828	0.182	0.199
$\mathrm{Re}(d)[t^{-2}]$	0.049	0.029	0.030
$\mathrm{Im}(d)[t^{-2}]$	0.547	0	0
$b[t^{-3}]$	2.246	0.184	0.217

coefficient a decreases with T, but it is more weakly T dependent than for weak coupling, i.e., when we set $\Delta = 0$ in Eq. (22). Second, for the value $U = 4t$, which is underlying our calculations, $a(T)$ clearly shows the tendency to vanish for $T \searrow T_c$. As discussed in Sec. III A in connection with the Thouless criterion,[31] this fact is directly related to the occurrence of the superconducting phase transition. Therefore, the temperature at which the system makes the transition to superconductivity is coinciding with the temperature at which the pseudogap is fully developed. We can thus conclude that our evaluation of the coefficients $a - d$, based on the simple form (27) for the electronic line shape yields a satisfactory self-consistency. This approach is, however, not able to give precisely the value of a for $T = T_c$ and we will use another way to determine it more accurately in Sec. IV B.

2. Coefficient d

Expression (24) yields $\mathrm{Re}(d) = 0.031t^{-2}$ for $T = T_c$, whereas the imaginary part $\mathrm{Im}(d)$ becomes very small when the pseudogap is fully developed, since it is directly proportional to the value of $\tilde{D}_{a,1}(\omega = 0)$, which then goes to zero. Thus, close to the transition temperature, the pairs acquire an increasingly long lifetime and, therefore, constitute well-defined bosonic quasiparticles.

3. Coefficient c

Expression (23) yields $c = 0.19t^{-1}$. According to our form (10) for the "pair propagator," one can attribute an effective mass
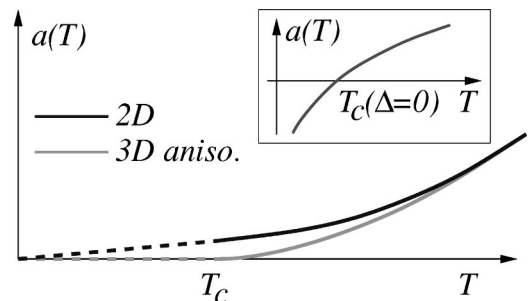
$$m_b = \frac{\mathrm{Re}(d)}{2c} \tag{52}$$

FIG. 4. Schematic temperature dependence of the coefficient a in various cases: strictly two-dimensional system, anisotropic three-dimensional system and, in the inset, weak-coupling regime.

to the virtual bosonic pairs. The corresponding value is $m_b = 0.16m$, the latter quantity m being the effective mass of the tight-binding electrons given by

$$m = \frac{1}{2t}. \tag{53}$$

A similar value for the bosonic effective mass has been found by Haussmann[36] and Stinzing and Zwerger.[19] At first sight this value of m_b seems rather small. However, we recall that the choice of the coupling $U = 4t$ represents an intermediate regime where the coherence length is of the order of the lattice constant. This means that the electronic pairs are not yet strongly localized at the lattice sites and that their effective mass is still lower than that in the large-U limit where it is of the order of $U/4t^2$.[30] Moreover, one should make a clear distinction between the effective curvature of the "bosonic band" near the origin in $\mathbf{k}$ space, as it is given by the coefficient c and thus by m_b, and the full width of this band. The latter can be estimated from the value of the T matrix (2) for $\mathbf{k} = (\pi, \pi)$. Indeed, inserting the noninteracting G_0 into Eq. (3), one finds that T has a pole for a real frequency, which is the so-called η peak,[20]

$$z_\eta = -(1-n)U - 2\mu. \tag{54}$$

Since, near T_c, the coefficient a is very small, the pole of T at $k = 0$ is directly at $z = 0$, and thus the effective bosonic bandwidth is directly given by Eq. (54), which for our case is on the order of $3.8t$. Using a BCS form for G with a finite width Γ, instead of G_0, requires a numerical calculation whose result is similar: the η peak is located at $z_\eta \approx 3.5t$. These values show that the bosonic bandwidth is indeed smaller than the noninteracting electronic bandwidth $W = 8t$, and it is compatible with numerical T-matrix results.[15]

4. Coefficient b

The result of the calculation of expression (45) using the spectral functions (27) is given in Appendix D. Although it is quite complicated, the expression giving the coefficient b can be interpreted in the same way as in the weak-coupling case ($\Gamma = \Delta = 0$). Thus b is essentially the sum of integrals containing the product of a weighted density of states with a function that is strongly peaked around the Fermi energy. Therefore, it becomes small when the pseudogap develops: for $\beta = T_c^{-1} = 15t^{-1}$ we find the value $b \approx 0.217t^{-3}$, which is one order of magnitude smaller than the weak-coupling result $7\zeta(3)\beta^2 D_0(\mu)/8\pi^2 \approx 2.24t^{-3}$ given in the literature.[14] This means that the interaction between the bosonic fluctuations weakens when the pseudogap approaches its full depth and becomes negligible close the superconducting transition, justifying the assumptions made previously (Sec. III E).

B. Number equation and "consistency checks"

We can now come back to the number equation (41) in order to estimate the number of preformed pairs near T_c. As already mentioned, the two terms entering this relation have a simple meaning: the total number of charge carriers is split up into nonpaired electrons (n_0) and fluctuating pairs (n_d).

The latter is given by a sum over all momenta of the pairs, weighted by the derivative of the pair energy $\Omega(\mathbf{k})$, given by Eq. (48), with respect to the (fermionic) chemical potential μ. Near T_c the dominant term is the contribution at $\mathbf{k} = 0$, that is the one proportional to $\partial a/\partial\mu$. Considering expressions (22) and (24) it is easy to see that

$$-\frac{\partial\Omega_{k=0}}{\partial\mu} = -\frac{1}{\text{Re}(d)}\frac{\partial a}{\partial\mu} = 2 \tag{55}$$

and, therefore, the second term in Eq. (41) is nothing else than twice the number n_b of pairs defined as expected by

$$n_b = \frac{1}{\text{Re}(d)N}\sum_{\mathbf{k}} n_B(\Omega_{\mathbf{k}}). \tag{56}$$

According to Eq. (42) the density n_0 of unpaired electrons per site is estimated by integrating the noninteracting (tight-binding) density of states $D_0(\epsilon)$ up to the (true) chemical potential $\mu = -3.5t$. This yields

$$n_0 = 0.1. \tag{57}$$

This value allows to find the number of pairs that is given by half of the number of "available" electrons,

$$n_b = \frac{n - n_0}{2} = 0.05. \tag{58}$$

This means that roughly one-half of the charge carriers contribute to the (virtual) pairing fluctuations. As illustrated in Fig. 3, this splitting of the total number of electrons into paired and unpaired particles is determined here by the value of the chemical potential μ. This is rather different from the BCS weak-coupling superconductivity, where the gap parameter Δ plays this role.

It is now possible to calculate precisely the (small) value of the coefficient a as announced above. First, we analytically evaluate the $\mathbf{k}$ sum in Eq. (56) and get

$$n_b = -\frac{1}{4\pi\beta c}\ln\left\{1 - \exp\left[-\frac{\beta a}{\text{Re}(d)}\right]\right\}. \tag{59}$$

Then, using the known values for β, c, and d, this equation is compared with Eq. (58) and solved for a. The result is $a = 2.78 \times 10^{-4}t^{-1}$ which is indeed too small to be obtained by the approach developed in Sec. III.

Now we want to see whether the value of n_b really makes sense by subjecting it to various "consistency checks" based on alternative approaches that are valid in similar situations:

(1) In its simplified form (15) the electronic self-energy leads to a simple relation between the pseudogap width 2Δ and the number of bosonic pairs: according to Eq. (10) the sum over wave vectors and Matsubara frequencies on the right-hand side of Eq. (16) is directly related to the number of pairs, provided that $\text{Im}(d)$ is small,

$$\frac{1}{\beta N}\sum_{\mathbf{k}, z_\alpha} T(\mathbf{k}, z_\alpha) = \frac{n_b}{\text{Re}(d)}. \tag{60}$$

Thus, given Eqs. (16) and (17), the following relation between the pseudogap half-width Δ and the number of pairs holds:

$$n_b = \mathrm{Re}(d)\left(\Delta^2 + \frac{\Gamma_0^2}{4}\right). \qquad (61)$$

Using $\mathrm{Re}(d) = 0.031 t^{-2}$, $\Delta = 0.5t$, and $\Gamma_0 = 0.125t$, we obtain $n_b = 0.008$, which is more than a factor 5 smaller than the value coming from the number equation. This discrepancy is due to replacing the full expression (14) for the electronic self-energy by the approximate form (15) which is only valid at weak coupling where the shift $\mu - \mu_0$ of the chemical potential is small (see Fig. 3) and which is definitely not suited for the case $U = 4t$.

(2) Stinzing and Zwerger[19] considered the BCS-BEC crossover problem at the level of a Gaussian approximation for the pairing field. Although their approach is devoted to the case of d-wave symmetry, we have already seen that it yields a value for the bosonic mass m_b which is similar to ours. For such a m_b value, their estimate for n_d is approximately equal to one-third of the total density of electrons n. In terms of the bosonic density, this gives $n_b = 0.033$ that is already closer to the value (58) found in the framework of our approach. The same result is obtained from Haussmann's work[36] that provides a value for the chemical potential shift (51):

$$\frac{\tilde{\mu}}{\tilde{\mu}_0} \approx \frac{n_0}{n} = \frac{2}{3}. \qquad (62)$$

Here the tilde ($\tilde{\ }$) means the value with respect to the bottom of the free band.

(3) One can also establish a link between n_b and the double occupancy n_2 of a given lattice site, which can be calculated by dividing the total potential energy by U [see expression (1) for the Hamiltonian]. This relation reads

$$n_2 = \left(\frac{n}{2}\right)^2 + n_b, \qquad (63)$$

where the first term represents the free electron contribution that is nonzero even without the attractive interaction. Our QMC results[37] are $n_2 = 0.05$ for $n = 0.2$ and $\beta = 15t^{-1}$. This corresponds to a value $n_b = 0.04$ which is satisfactorily close to the one obtained with our approach. We should mention that n_b was defined here as the expectation value of the operator $\Sigma_i (c_{i\uparrow} c_{i\downarrow})^\dagger (c_{i\uparrow} c_{i\downarrow})$ describing strictly local pairs. The latter may be different from the ones appearing in an intermediate coupling regime.

The conclusion of the above is that the order of magnitude of n_b is correct, maybe a bit overestimated. This is probably due to restricting the **k**-dependent weight factor in Eq. (47) to its value in $k = 0$ and to neglecting the bosonic interaction in Eq. (46). Indeed, it has been shown that the latter may lead to a depletion of the number of bosons to a slightly lower value.[17,30] However, our estimate of the bosonic density remains valid and fully compatible with the idea of preformed local pairs existing above the critical temperature.

C. Influence of a weak interplane coupling

For a 3D anisotropic system, one has to add a term to the Hamiltonian (1) that describes hopping between neighboring lattice planes involving the hopping amplitude $t_\perp$. The ratio between the two parameters

$$\gamma^2 = \frac{t}{t_\perp} \qquad (64)$$

defines the electronic anisotropy. When the tight-binding spectrum is approximated by a quadratic form for small wave vectors, γ^2 can be expressed by the product of the lattice anisotropy times the ratio between the electronic effective masses m and $m_\perp$. The T-matrix expressions (2)–(5) remain valid, the wave-vector sum now running over the 3D Brillouin zone. However, rather than performing these 3D sums explicitly, we estimate in a simple way the effect of the additional sum over the z component of the wave vectors on the results obtained up to this point for a strictly 2D system.

It is clear that this additional sum over the perpendicular direction "smears out" the form of χ and σ, obtained through Eqs. (2) and (5). Therefore, its main effect can be summarized by introducing an additional contribution $\Gamma_\perp$ to the spectral linewidth of the corresponding quantity, obtained previously by a 2D wave-vector sum.

Following again the approximate scheme developed in Secs. III A–III C, one first has to evaluate the electronic self-energy according to Eq. (14). The effect of summing also over the z component of the wave vector **q** is incorporated in σ by increasing its linewidth. An upper limit for the corresponding $\Gamma_\perp$ should be given by the sum of the total variation of the two factors in Eq. (14) over the domain of q_z, i.e., the maximum value of the band dispersion in z direction

$$\Gamma_\perp \lesssim 2t_\perp \qquad (65)$$

and the additional width of the "bosonic band" given by $\mathrm{Im}[T(\mathbf{q}, z_\alpha)]$. Given that the estimate (54) is also valid for the η peak in 3D, we can neglect the difference in the bosonic bandwidth between 2D and 3D, and thus our estimate of $\Gamma_\perp$ for σ is directly given by Eq. (65). According to Ref. 28, the linewidth of $\sigma(\mathbf{q}, z_\nu)$ near the Fermi surface is on the order of $0.2t$. Thus, the additional broadening has a small effect provided that

$$\frac{2t_\perp}{0.2t} = \frac{10}{\gamma^2} \ll 1. \qquad (66)$$

For the next step, the evaluation of the T-matrix coefficients performed in Sec. III C for 2D, we simply add the linewidth (65) to the linewidth Γ that characterized our approximate electronic spectral function (27) in the pseudogap regime. Then the 3D effects are small as long as

$$2t_\perp \ll \Gamma. \qquad (67)$$

Given our choice of $\Gamma = t/8$, the inequalities (66) and (67) are satisfied and the pseudogap should not be appreciably affected by the weak interplane coupling, as long as

$$\gamma^2 \gg 16. \qquad (68)$$

This requirement is in agreement with other authors[38] who claim that the pseudogap is a typical 2D phenomenon since in this case the pairing fluctuations are strongly enhanced.[24] On the other hand, the latter become much weaker when one approaches the 3D anisotropic case where the pseudogap should then be observable only very close to T_c. There are, however, several nontrivial features resulting from the weak interlayer coupling, which we will mention now. A quantitative analysis would be delicate within our approach since the result would depend rather sensitively on the interplay between two small parameters, namely, the linewidth Γ and the additional bandwidth $2t_\perp$. Therefore, we restrict ourselves to qualitative considerations and eventually borrow some results from other studies.

The following two quantities are affected by the weak interlayer coupling:

(1) *Coefficient a*. Unlike the strictly 2D case, the transition to the superconducting phase transition must now satisfy the Thouless criterion as mentioned above. Thus, $a(T)$ must vanish at $T = T_c$ as sketched in Fig. 2.

(2) *Coefficient c*. There is now an additional parameter, namely, a coefficient $c_\perp$ that multiplies k_z^2 in the T matrix (10). This quantity allows to define the bosonic anisotropy as

$$\gamma_b^2 = \frac{c}{c_\perp}. \tag{69}$$

Since it describes the correlated motion of two electrons along the z direction, it is different (and in fact much larger) than the single electronic anisotropy γ^2. In a similar context, Quick and Sharapov[39] derived the following expression for quasi-2D systems,

$$\gamma_b^2 = 2\pi n\, \gamma^4, \tag{70}$$

where n is the electronic density.

It is now possible to apply the above considerations to real (3D) materials in order to determine the circumstances under which the bosonic properties associated with the T matrix may be observed. It appears that the bosonic anisotropy γ_b defined above can be written as a product,

$$\gamma_b = \lambda \gamma_m, \tag{71}$$

where λ is the lattice anisotropy (out-of-plane lattice constant divided by in-plane lattice constant) and γ_m the "bosonic mass" anisotropy that can be extracted from penetration depth measurements. The data for the bilayered compound Bi-2212 ($\lambda = 30.7/2 \times 5.4 \sim 3$, $\gamma_m \sim 200$ and $n \sim 0.1$) give $\gamma_b \sim 600$. Using Eq. (70), we get $\gamma^2 \sim 750$ that satisfies the above conditions (66) and (68). Thus, we may understand the observation of typical BEC features in the specific-heat measurements of underdoped BSCCO.[1] On the other hand, the corresponding parameters for underdoped YBCO ($\lambda \sim 11.7/2 \times 3.8 \sim 1.5$ and $\gamma_m \sim 30$) yield $\gamma^2 \sim 55$. This value does not fulfill the above requirements and the BEC properties are "smeared out" by the interlayer coupling to give finally the XY-like behavior that has been observed experimentally.[1]

D. The superconducting transition as a Bose-Einstein condensation

An important confirmation of the consistency of our approach was provided by the fact that the critical temperature $T_c \approx t/15$ was found to correspond to the point where the coefficient a showed clearly the tendency to become very small (and eventually to vanish in 3D). This agreed with the Thouless criterion for superconductivity. The interpretation of the T matrix as the propagator of well-defined noninteracting bosonic quasiparticles may suggest that one should be able as well to view the transition to the superconducting state as a condensation of these bosons, forgetting completely about the underlying electrons. In that case, the critical temperature T_c should correspond to the BEC transition temperature of the bosons described by the T matrix.

A first step in this direction was already performed in the previous section where we have introduced a weak interlayer coupling, making our system three-dimensional. This enables a finite-temperature condensation of the noninteracting bosons. In order to preserve the main properties deduced for the strictly two-dimensional case (and displaying typical BEC features), we imposed conditions on the electronic anisotropy constant γ. According to Sec. IV C typical values $\gamma_b \sim 500$–1000 are well suited to describe underdoped high-temperature superconductors such as BSCCO. In this case, we expect the following relation to hold:

$$T_{c,\mathrm{BEC}} \gg \frac{c}{\gamma_b^2 \,\mathrm{Re}(d)}. \tag{72}$$

This situation corresponds to the case of "strongly anisotropic" bosons for which an implicit expression for the critical temperature $T_{c,\mathrm{BEC}}$ has been derived by Wen and Kan.[40] It reads

$$T_{c,\mathrm{BEC}} = 4\pi n_b \frac{c}{\mathrm{Re}(d)} \left/ \ln\left[T_{c,\mathrm{BEC}} \frac{\gamma_b^2 \,\mathrm{Re}(d)}{c} \right] \right.. \tag{73}$$

All the parameters entering the above formula have been determined previously so that we may use it straightforwardly to see whether the system we are considering really consists in free bosons undergoing a BEC. The result is

$$T_{c,\mathrm{BEC}} = 0.4t. \tag{74}$$

This shows clearly that Eq. (73) gives a value that is substantially larger than the "true" critical temperature $T_c \approx 0.07t$ obtained from other methods.[22,35] It could be lowered to T_c by the choice of a higher anisotropy ($\gamma_b \sim 10^7$) but the latter would become so large that it would be meaningless to speak about a 3D system. Therefore, this discrepancy is an intrinsic feature of the intermediate coupling range of the model. This is confirmed by applying the same procedure to the 3D isotropic case considered by Haussmann[36] where, after using the usual formula for $T_{c,\mathrm{BEC}}$,[26] a similar disagreement between the true transition temperature and the BEC value is found as well.

It is clear that the coupling strength $U = 4t$ represents an intermediate regime for which the pure BEC physics valid for large U is not expected to work. However, the study of

the T matrix performed above has shown that the latter could be legitimately interpreted as the propagator of well-defined noninteracting bosons approaching a BEC as $T \searrow T_c$. The observed inadequacy of the BEC critical temperature means that the "unpaired" electrons cannot be omitted. Although their contribution to the thermodynamic potential (30) is uninteresting, they still play a role in inhibiting the bosonic states to arrange themselves to form the BE condensate as if they were alone. It is thus normal that the true critical temperature lies below the one predicted by the BEC scenario. They will coincide once the effects of the "unpaired" electrons have disappeared, i.e., when $n_0 = 0$, what corresponds to the strong-coupling regime where *all* the electrons are forming the $n_b = n/2$ pairs.

It is interesting to note that the evaluation of the formula (73) with the incorrect (asymptotic) bosonic parameters $n_b = n/2 = 0.1$ and $c/\mathrm{Re}(d) = 2t^2/U = 0.5t$ yields $T_{c,\mathrm{BEC}} = 0.06t$, which is very close to the true $T_c \approx 0.07t$. Such a procedure was used in Ref. 1 and gave, together with the shapes of the specific-heat curves, a strong experimental support for the interpretation of the superconducting transition in underdoped high-temperature superconductors such as BSCCO as a BEC. In the light of the present work, the agreement between these two aspects seems to be the result of a coincidence rather than the manifestation of an authentic BEC of preformed pairs.

V. SUMMARY

We have studied the attractive Hubbard model (1) on a strongly anisotropic lattice for an attraction strength of the order of half the free-electron bandwidth by means of the T-matrix approximation. We have focused on the temperature regime close to, but above the superconducting transition temperature T_c, where a pseudogap is developing in the one-electron density of states.

An approximate self-consistency in the solution of equation (2)–(5), determining the relevant quantities of the T-matrix approach, has been achieved by proceeding in two steps. The first step—a perturbative calculation of the one-electron Green function by approximating the full Green function in Eq. (5) by its free-electron form, and the T matrix $T(\mathbf{q}, z_\nu)$ by its form for small wave vectors $\mathbf{q}$ and frequencies z_ν—has been taken over from previous work.[28] The resulting spectral function has been approximated by a BCS form with an energy-dependent linewidth. The second step consists in (re)calculating the coefficients determining $T(\mathbf{q}, z_\nu)$ by using these broadened BCS spectral functions in Eq. (3) for the "factorized particle-particle susceptibility" χ that yields $T(\mathbf{k}, z_a)$ according to Eq. (2). As a result, we confirmed the superconducting transition temperature through the Thouless criterion: $T(0,0)$ diverges for temperatures $T \searrow T_c$. As a next step, we have studied, still in the framework of the T-matrix approximation, the thermodynamic properties of the model in the pseudogap regime, namely, the grand canonical potential and the "number equation" determining the link between the electron density and the chemical potential. Close to T_c, the number equation reduces to a simple form, which says that the total particle number is approximately equal to the

sum of the number of "unpaired" electrons and twice the number of "virtual pairs." The lifetime of the latter, which have bosonic properties, becomes longer and longer, and their interaction weaker and weaker, when T_c is approached. The fraction of electrons that participate in the constitution of these "preformed" pairs is estimated by different approximate relations. It is on the order of one half.

At the end of these calculations that are performed for a strictly 2D system representing one lattice plane, the influence of a weak interplane coupling is estimated. In agreement with other works, it is found that the pseudogap scenario should not be substantially altered, as long as the hopping of electrons from one plane to the other is sufficiently weak. However, on the formal side, a nonvanishing interplane coupling is necessary in order to be able to treat the superconducting transition either as a "normal" XY transition or as a Bose-Einstein condensation, whereas in a truly 2D system one would expect a Kosterlitz-Thouless scenario, which is more difficult to describe in a perturbative approach.

We finally use the quantities that characterize the bosonic pairs in order to calculate the critical temperature of the BEC associated to the latter. The obtained value appears to be definitively larger than the "true" critical temperature. This shows that, for an intermediate coupling, a description of the superconducting transition in terms of bosons only is incomplete: unpaired electrons cannot be omitted although they do not contribute explicitly to the part of the thermodynamic potential that is relevant as $T \searrow T_c$. On the other hand, the "true" critical temperature—given by the Thouless criterion of a diverging T matrix (in which all electrons are involved)—can be equivalently reformulated as the point where the chemical potential associated with the bosons described by the T matrix is vanishing, which is a fundamental feature of a BEC. In this context, it then seems natural to understand observations, like the specific heat of strongly anisotropic high-temperature superconductors,[1] as a sign of Bose-Einstein physics.

Summarizing, we have interpreted the physical properties of a strongly anisotropic superconductor, described by the attractive Hubbard Hamiltonian, in its normal state close to the critical temperature, in terms of a "two-fluid" picture of coexisting preformed pairs and unpaired electrons. Various authors have analyzed the properties of such a system by working directly with a Hamiltonian of coupled fermions and bosons.[41] The self-consistent T-matrix approximation used in this work has the advantage that one can start from a purely electronic model (albeit with an electronic attraction with unspecified origin). The formal expressions determining the thermodynamic and the one-electron properties then lead in a natural way to the two-fluid picture and allows us to determine the relevant parameters that characterize the bosons.

APPENDIX A: CALCULATION OF THE COEFFICIENTS a, c, AND d BY USING SPECTRAL FUNCTIONS

Expressions (11)–(13) for the coefficients a, c, and d are based on the particle-particle bubble $\chi(\mathbf{k}, z_\alpha)$ from Eq. (3). We first reexpress it in terms of the spectral function $A(\mathbf{k}, \omega)$ by using the Lehmann representation for the Green function:[26]

$$G(\mathbf{k}, z_\nu) = \frac{1}{2\pi} \int d\omega \frac{A(\mathbf{k}, \omega)}{z_\nu - \omega}. \tag{A1}$$

This gives

$$\chi(\mathbf{k}, z_\alpha) = \frac{1}{\beta} \sum_{z_\nu} \int d\omega d\omega'$$

$$\times \frac{1}{(z_\alpha - z_\nu) - \omega} \frac{1}{z_\nu - \omega'} \phi(\mathbf{k}, \omega, \omega'), \tag{A2}$$

where

$$\phi(\mathbf{k}, \omega, \omega') = \frac{1}{(2\pi)^2} \frac{1}{N} \sum_{\mathbf{q}} A(\mathbf{k} - \mathbf{q}, \omega) A(\mathbf{q}, \omega'). \tag{A3}$$

Performing the frequency summation in Eq. (A2) yields[26]

$$\chi(\mathbf{k}, z_\alpha) = -\int d\omega d\omega' \frac{1 - n_F(\omega) - n_F(\omega')}{z_\alpha - (\omega + \omega')} \phi(\mathbf{k}, \omega, \omega'), \tag{A4}$$

where n_F is the Fermi-Dirac distribution

$$n_F(\omega) = \frac{1}{e^{\beta\omega} + 1}. \tag{A5}$$

Now we can introduce the explicit expression of the spectral function in order to evaluate the quantity $\phi(\mathbf{k}, \omega, \omega')$. As a first step, we take the BCS expression (18). The generalization to the pseudogap regime we are interested in will be straightforward as shown in Appendix C. For simplicity, we consider the case $\mathbf{k} = 0$, which concerns the coefficients a and d. But this method also applies to c once the two k derivations have been performed and the derivatives of the δ functions have been removed by partial integrations over ω. Inserting expression (18) into Eq. (A3) gives

$$\phi(0, \omega, \omega') = \frac{1}{N} \sum_{\mathbf{q}} \{u_{\mathbf{q}}^4 \delta(E_{\mathbf{q}} - \omega) \delta(E_{\mathbf{q}} - \omega')$$

$$+ v_{\mathbf{q}}^4 \delta(E_{\mathbf{q}} + \omega) \delta(E_{\mathbf{q}} + \omega')$$

$$+ u_{\mathbf{q}}^2 v_{\mathbf{q}}^2 \delta(E_{\mathbf{q}} - \omega) \delta(E_{\mathbf{q}} + \omega')$$

$$+ u_{\mathbf{q}}^2 v_{\mathbf{q}}^2 \delta(E_{\mathbf{q}} + \omega) \delta(E_{\mathbf{q}} - \omega')\}. \tag{A6}$$

Using the property $\delta(x - a) \delta(x - b) = \delta(x - a) \delta(a - b)$, we find

$$\phi(0, \omega, \omega') = \delta(\omega - \omega') D_{a,1}\left(\frac{\omega + \omega'}{2}\right)$$

$$+ \delta\left(\frac{\omega + \omega'}{2}\right) D_{a,2}(\omega - \omega'), \tag{A7}$$

where

$$D_{a,1}(\omega) = \frac{1}{N} \sum_{\mathbf{q}} [u_{\mathbf{q}}^4 \delta(E_{\mathbf{q}} - \omega) + v_{\mathbf{q}}^4 \delta(E_{\mathbf{q}} + \omega)], \tag{A8}$$

$$D_{a,2}(\omega) = \frac{1}{N} \sum_{\mathbf{q}} u_{\mathbf{q}}^2 v_{\mathbf{q}}^2 [\delta(E_{\mathbf{q}} - \omega) + \delta(E_{\mathbf{q}} + \omega)]. \tag{A9}$$

Now we can perform the $\mathbf{q}$ integration in the above expressions by introducing the tight-binding density of states

$$D_0(\epsilon) = \frac{1}{N} \sum_{\mathbf{q}} \delta(\varepsilon_{\mathbf{q}} - \epsilon) = \frac{1}{2\pi} F\left[\frac{\pi}{2}, \sqrt{1 - (\epsilon/[W/2])^2}\right], \tag{A10}$$

where F is the elliptic integral of the first kind. Integration over $\epsilon = \mu + \xi$ gives the final expressions for $D_{a,1}$ and $D_{a,2}$ displayed in Appendix B. The contribution (A9) is often referred to as "Landau term" and describes interband effects.

The coefficients a, c, and d are obtained from Eq. (A4) that can be still simplified by making the variable transformation $(\omega, \omega') \rightarrow (\Omega = (\omega + \omega')/2, \theta = \omega' - \omega)$, as suggested by Eq. (A7). This allows us to eliminate one of the integrals in Eq. (A4) and to finally obtain the expressions given in Appendix B.

APPENDIX B: RESULTS FOR BCS SPECTRAL FUNCTIONS

In the following, we give the exact expressions for the coefficients a, c, and d defined in Eqs. (11)–(13) and calculated them using the method of Appendix A based on the BCS spectral functions (18). They read

$$a = \frac{1}{U} - \int d\omega \left\{ D_{a,1}(\omega) \frac{\tanh(\beta\omega/2)}{2\omega} - D_{a,2}(\omega) n_F'(\omega) \right\}, \tag{B1}$$

$$c = \int d\omega \left\{ D_{c,11}(\omega) \frac{\tanh(\beta\omega/2)}{2\omega} \right.$$

$$+ D_{c,31}(\omega) \left[\frac{\tanh(\beta\omega/2)}{4\omega^2} + \frac{n_F'(\omega)}{2\omega} \right]$$

$$+ D_{c,51}(\omega) \left[-\frac{\tanh(\beta\omega/2)}{4\omega^3} - \frac{n_F'(\omega)}{2\omega^2} + \frac{n_F''(\omega)}{2\omega} \right] \right\}$$

$$\times \frac{1}{2} \left(\frac{d\xi_{\mathbf{k}}}{dk}\right)^2_{k=k(\omega)}$$

$$+ \int d\omega \left\{ D_{c,12}(\omega) \frac{\tanh(\beta\omega/2)}{2\omega} \right.$$

$$+ D_{c,32}(\omega) \left[\frac{\tanh(\beta\omega/2)}{4\omega^2} + \frac{n_F'(\omega)}{2\omega} \right] \right\} \left(\frac{d^2\xi_{\mathbf{k}}}{dk^2}\right)_{k=k(\omega)}, \tag{B2}$$

$$d = \mathcal{P} \int d\omega D_{a,1}(\omega) \frac{\tanh(\beta\omega/2)}{4\omega^2} + i\frac{\pi}{8}\beta D_{a,1}(0), \quad \text{(B3)}$$

where the "weighted" density of states are given by

$$D_{a,1}(\omega) = D_{\text{BCS}}(\omega)\left(1 - \frac{\Delta^2}{2\omega^2}\right), \quad \text{(B4)}$$

$$D_{a,2}(\omega) = D_{\text{BCS}}(\omega)\frac{\Delta^2}{2\omega^2}, \quad \text{(B5)}$$

$$D_{c,11}(\omega) = D_{\text{BCS}}(\omega)\frac{3\Delta^2}{4\omega^2}\left(-1 + \frac{\Delta^2}{\omega^2}\right), \quad \text{(B6)}$$

$$D_{c,12}(\omega) = D_{\text{BCS}}(\omega)\frac{\Delta^2}{4\omega^4}\xi(\omega), \quad \text{(B7)}$$

$$D_{c,31}(\omega) = D_{\text{BCS}}(\omega)\frac{\Delta^2}{\omega^3}\left(1 - \frac{3\Delta^2}{4\omega^2}\right), \quad \text{(B8)}$$

$$D_{c,32}(\omega) = D_{\text{BCS}}(\omega)\frac{\xi(\omega)}{2\omega}\left(1 - \frac{\Delta^2}{2\omega^2}\right), \quad \text{(B9)}$$

$$D_{c,51}(\omega) = D_{\text{BCS}}(\omega)\left(\frac{1}{2} - \frac{3\Delta^2}{4\omega^2} + \frac{\Delta^4}{4\omega^4}\right), \quad \text{(B10)}$$

and contain the BCS expressions

$$D_{\text{BCS}}(\omega) = D_0[\mu_0 + \xi(\omega)]\varrho(\omega) \quad \text{(B11)}$$

$$\xi(\omega) = \text{sgn}(\omega)\sqrt{\omega^2 - \Delta^2} \quad \text{(B12)}$$

$$\varrho(\omega) = \frac{|\omega|}{\sqrt{\omega^2 - \Delta^2}}. \quad \text{(B13)}$$

Equations (22) and (23) are a bit different from the above expressions (B1) and (B2) because negligible terms are omitted and the derivatives of the bare dispersion $\xi_{\mathbf{k}}$ are factored out from the integrals in order to make their evaluation easier.

APPENDIX C: BROADENED BCS SPECTRAL FUNCTIONS

Here we show how to modify the method and the results shown in Appendixes A and B in order to calculate the coefficients a, c, and d for the spectral functions given by Eq. (27). First, the property of the δ functions used to derive Eq. (A7) is no longer true. However, it is possible to obtain approximately a similar result by using the following strategy. We introduce the variables transformation $(\omega, \omega') \rightarrow (\Omega, \theta)$ defined in Appendix A in Eq. (A6) and assume that the functions f_Γ can be approximated by a Gaussian distribution as defined in Eq. (28). This is quite reasonable as long as we

have very peaked line shapes, i.e., $\Gamma \ll W$. Then we have, for example,

$$f_\Gamma(E_{\mathbf{q}} - \omega)f_\Gamma(E_{\mathbf{q}} - \omega') = f_{\Gamma/\sqrt{2}}(E_{\mathbf{q}} - \Omega)f_{\sqrt{2}\Gamma}(\theta), \quad \text{(C1)}$$

which yields an expression for $\phi(0,\omega,\omega')$ similar to Eq. (A7). For simplicity, we take $f_{\Gamma/\sqrt{2}} \approx f_{\sqrt{2}\Gamma} \approx f_\Gamma$. The next step is the integration over the variable θ, which can be achieved by expanding the fraction in Eq. (A4) with respect to the latter and keeping only the zeroth-order term. The first corrections are of second order and can be safely neglected for our purposes. Thus we finally get expressions for the coefficients a, c, and d, which are very similar to those calculated for the BCS case. This is the main advantage of our method. The only difference lies in the "weighted" density of state functions (B4)–(B10), which must be modified according to

$$D_{a,1}(\omega) \rightarrow \tilde{D}_{a,1}(\omega) \equiv \int dE D_{a,1}(E)f_\Gamma(E - \omega), \quad \text{(C2)}$$

for example. We shall use a tilde $\tilde{D}$ to refer to the case of "broadened" density of states corresponding to the spectral function (27).

APPENDIX D: EVALUATION OF THE COEFFICIENT b

In this section, we present the result of the calculation of the coefficient b giving the strength of the bosonic interaction. Proceeding as explained in the previous appendices, we find the following expression:

$$b = \int d\omega D_{\text{BCS}}(\omega)[u_\omega^4 \tilde{H}_{uu}(\omega) + v_\omega^4 \tilde{H}_{vv}(\omega) + 2u_\omega^2 v_\omega^2 \tilde{H}_{uv}(\omega)]. \quad \text{(D1)}$$

Here the finite width Γ of the spectral functions manifests itself as

$$\tilde{H}_{uu}(\omega) = \int d\Omega f_\Gamma(\Omega - \omega)H[\Omega, \xi(\omega)], \quad \text{(D2)}$$

$$\tilde{H}_{vv}(\omega) = \int d\Omega f_\Gamma(\Omega + \omega)H[\Omega, \xi(\omega)], \quad \text{(D3)}$$

$$\tilde{H}_{uv}(\omega) = \int d\theta f_\Gamma(\theta - \omega)\frac{1}{\theta}\{H_L[\theta, \xi(\omega)] - H_L[-\theta, \xi(\omega)]\}, \quad \text{(D4)}$$

and the corresponding expressions for the BCS case are

$$H(\omega_1, \omega_2) = 2\frac{1 - n_F(\omega_1) - n_F(\omega_2)}{(\omega_1 + \omega_2)^3} + \frac{n_F'(\omega_1) + n_F'(\omega_2)}{(\omega_1 + \omega_2)^2}, \quad \text{(D5)}$$

$$H_L(\omega_1, \omega_2) = -\frac{1 - n_F(\omega_1) - n_F(\omega_2)}{(\omega_1 + \omega_2)^2} - \frac{n_F'(\omega_2)}{\omega_1 + \omega_2}. \quad \text{(D6)}$$

[1] A. Junod, A. Erb, and Ch. Renner, Physica C **317-318**, 333 (1999).

[2] A. S. Alexandrov, W. H. Beere, V. V. Kabanov, and W. Y. Liang, Phys. Rev. Lett. **79**, 1551 (1997).

[3] See, e.g., H. Ding, T. Yokoya, J. C. Campuzano, T. Takahashi, M. Randeria, M. R. Norman, T. Mochiku, K. Kadowaki, and J. Giapintzakis, Nature (London) **382**, 52 (1996); A. G. Loeser, Z. X. Shen, D. S. Dessau, D. S. Marshall, C. H. Park, P. Fournier, and A. Kapitulnik, Science **273**, 325 (1996); M. R. Norman, H. Ding, M. Randeria, J. C. Campuzano, T. Yokoya, T. Takeuchi, T. Takahashi, T. Mochiku, K. Kadowaki, P. Guptasarma, and D. G. Hinks, Nature (London) **392**, 157 (1998); and references therein.

[4] Ch. Renner, B. Revaz, K. Kadowaki, I. Maggio-Aprile, and Ø Fischer, Phys. Rev. Lett. **80**, 3606 (1998).

[5] For a recent review see, e.g., T. Timusk and B. Statt, Rep. Prog. Phys. **62**, 61 (1999).

[6] V. J. Emery and S. A. Kivelson, Nature (London) **374**, 434 (1995).

[7] V. M. Krasnov, A. Yurgens, D. Winkler, P. Delsing, and T. Claeson, Phys. Rev. Lett. **84**, 5860 (2000); M. Suzuki and T. Watanabe, *ibid.* **85**, 4787 (2000).

[8] J. L. Tallon and J. W. Loram, Physica C **349**, 53 (2001).

[9] Y. J. Uemura, A. Keren, L. P. Le, G. M. Luke, W. D. Wu, Y. Kubo, T. Manako, Y. Shimakawa, M. Subramanian, J. L. Cobb, and J. T. Markert, Nature (London) **364**, 605 (1993).

[10] R. Micnas, J. Ranninger, and S. Robaszkiewicz, Rev. Mod. Phys. **62**, 113 (1990).

[11] M. Randeria, in *Bose Einstein Condensation*, edited by A. Griffin, D. Snoke, and S. Stringari (Cambridge University Press, Cambridge, UK, 1994).

[12] F. Pistolesi and G. C. Strinati, Phys. Rev. B **53**, 15 168 (1996); M. Marini, F. Pistolesi, and G. C. Strinati, Eur. Phys. J. B **1**, 151 (1998).

[13] T. Meintrup, T. Schneider, and H. Beck, Physica C **235−240**, 2139 (1994); T. Meintrup, T. Schneider, and H. Beck, Europhys. Lett. **31**, 231 (1995); J. P. Wallington and J. F. Annett, Phys. Rev. B **61**, 1433 (2000).

[14] M. Drechsler and W. Zwerger, Ann. Phys. (Leipzig) **1**, 15 (1992); C. A. R. Sa de Melo, M. Randeria, and J. R. Engelbrecht, Phys. Rev. Lett. **71**, 3202 (1993).

[15] P. Nozières and S. Schmitt-Rink, J. Low Temp. Phys. **59**, 195 (1985); R. Frésard, B. Glasser, and P. Wölfle, J. Phys.: Condens. Matter **4**, 8565 (1992); R. Micnas, M. H. Pedersen, S. Schafroth,

[16] N. E. Bickers, D. J. Scalapino, and S. R. White, Phys. Rev. Lett. **62**, 961 (1989).

[17] B. L. Gyorffy, J. B. Staunton, and G. M. Stocks, Phys. Rev. B **44**, 5190 (1991).

[18] J. M. Singer, M. H. Pedersen, T. Schneider, H. Beck, and H. G. Mattutis, Phys. Rev. B **54**, 1286 (1996); J. M. Singer, T. Schneider, and P. F. Meier, Eur. Phys. J. B **7**, 37 (1999).

[19] S. Stinzing and W. Zwerger, Phys. Rev. B **56**, 9004 (1997).

[20] M. Y. Kagan, R. Frésard, M. Capezzali, and H. Beck, Phys. Rev. B **57**, 5995 (1998); Physica B **284−288**, 447 (2000).

[21] M. Randeria, N. Trivedi, A. Moreo, and R. T. Scalettar, Phys. Rev. Lett. **69**, 2001 (1992).

[22] J. W. Serene and D. W. Hess, Phys. Rev. B **44**, 3391 (1991).

[23] O. Tchernyshyov, Phys. Rev. B **56**, 3372 (1997).

[24] V. M. Loktev, R. M. Quick, and S. G. Sharapov, Phys. Rep. **349**, 1 (2001).

[25] L. P. Kadanoff and G. Baym, *Quantum Statistical Mechanics* (W. A. Benjamin, New York, 1962), Chap. 13.

[26] A. L. Fetter and J. D. Walecka, *Quantum Theory of Many-Particle Systems* (McGraw-Hill, New York, 1971).

[27] D. Foerster, Phys. Rev. B **61**, R5066 (2000).

[28] M. Capezzali and H. Beck, Physica C **317-318**, 418 (1999).

[29] D. Rohe and W. Metzner, Phys. Rev. B **63**, 224509 (2001).

[30] M. H. Pedersen, Ph.D. thesis, University of Zürich, 1996.

[31] D. J. Thouless, Ann. Phys. (N.Y.) **10**, 553 (1960).

[32] J. J. Deisz, D. W. Hess, and J. W. Serene, Phys. Rev. Lett. **80**, 373 (1998).

[33] H. T. C. Stoof, Phys. Rev. B **47**, 7979 (1993).

[34] E. M. Lifshitz and L. P. Pitaevski, *Statistical Physics*, Part 2 (Pergamon, Oxford, 1980), Chap. 30.

[35] S. Allen, H. Touchette, S. Moukouri, Y. M. Vilk, and A.-M. S. Tremblay, Phys. Rev. Lett. **83**, 4128 (1999); B. Kyung, S. Allen, and A.-M. S. Tremblay, Phys. Rev. B **64**, 075116 (2001).

[36] R. Haussmann, Phys. Rev. B **49**, 12 975 (1994).

[37] A. Sewer, Ph.D. thesis, Université de Neuchâtel, 2001.

[38] See, for example, H. C. Ren, Physica C **303**, 115 (1998).

[39] R. M. Quick and S. G. Sharapov, Physica C **301**, 262 (1998).

[40] X. G. Wen and R. Kan, Phys. Rev. B **37**, 595 (1988).

[41] J. Ranninger, J. M. Robin, and M. Eschrig, Phys. Rev. Lett. **74**, 4027 (1995); V. B. Geshkenbein, L. B. Ioffe, and A. I. Larkin, Phys. Rev. B **55**, 3173 (1997); P. Devillard and J. Ranninger, Phys. Rev. Lett. **84**, 5200 (2000).